Electronic Supplementary Material (ESI) for Journal of Materials Chemistry A.

Supporting Information

Homointerface covalent organic framework membranes for efficient desalination

Jianliang Shen,[ab#] Jinqiu Yuan,[ab#] Benbing Shi,[ab] Xinda You,[ab] Rui Ding,[ab] Tianyi Zhang,[ab] Yujing Zhang,[ab] Yuanzhi Deng,[ab] Jingyuan Guan,[ab] Mengying Long,[ab] Yu Zheng,[ab] Runnan Zhang,[*abc] Hong Wu[abe] and Zhongyi Jiang[*abcd]

[a] *Key Laboratory for Green Chemical Technology of Ministry of Education, School of Chemical Engineering and Technology, Tianjin University, Tianjin 300072, China.*

[b] *Collaborative Innovation Center of Chemical Science and Engineering (Tianjin), Tianjin 300072, China.*

[c] *Zhejiang Institute of Tianjin University, Ningbo, Zhejiang 315201, China.*

[d] *Joint School of National University of Singapore and Tianjin University, International Campus of Tianjin University, Binhai New City, Fuzhou 350207, China.*

[e] *Tianjin Key Laboratory of Membrane Science and Desalination Technology, Tianjin University, Tianjin 300072, China.*

[#] *These authors contributed equally to this work.*

[*] *E-mail address: zhyjiang@tju.edu.cn.(Z., Jiang)*

[*] *E-mail address: runnan.zhang@tju.edu.cn. (R., Zhang)*

1. Methods

1.1 Materials

All chemicals and solvents were commercially available and used as received. 2,5-Diaminobenzenesulfonic acid (DABA) was purchased from Saen chemical technology (Shanghai) Co., Ltd. 1,3,5-Triformylphloroglucinol (TFP) was supplied by Jilin Chinese Academy of Sciences-Yanshen Technology Co., Ltd. p-Phenylenediamine (PA), 1,3,5-trimethylbenzene and acetic acid were provided by Shanghai Aladdin Biochemical Technology Co., Ltd. Hydrazine hydrate (N_2H_4) was obtained from Tianjin Jiangtian chemical technology co., Ltd. Sodium sulfate (Na_2SO_4), magnesium sulfate ($MgSO_4$), magnesium chloride ($MgCl_2$) and sodium chloride (NaCl) were obtained from Tianjin Kemiou Chemical Reagent Co. Ltd. Dopamine hydrochloride was purchased from Shanghai Macklin Biochemical Co., Ltd. Tris(hydroxymethyl) aminomethane-hydrochloric acid buffer (Tris-HCl, 50.0 mM, pH=8.5) was purchased from Nanjing Senbeijia Biotech Co., Ltd. Deionized water (DI) was obtained from a Milli-Q reverse osmosis system (Millipore, US). Polyacrylonitrile supports (PAN, MWCO=100 kDa) were purchased from Lanjing Membrane Technology Co., Ltd (Shandong, China).

1.2 Characterization

SEM. The surface and cross-sectional morphologies of the membranes were conducted by a field emission scanning electron microscopy (Hitachi S4800, Japan). All the membrane samples were sputtered with Au by a Q150T turbo-pumped sputter coater with the current of 25 mA for 120 s before SEM characterization.

TEM. The cross-sectional images of the membranes were obtained by a transmission electron microscopy (JEOL-2100F, Japan). Membrane sample was embedded by epoxy resin and then cut into slices (about 100 nm in thickness) by an ultramicrotome (Leica Ultracut R). Then, a microgrid copper was used to load these slice-shaped samples.

AFM. Three-dimensional morphology of the surface of COF membranes was characterized by Atomic force microscopy (AFM, NTEGRA spectra, Russia).

Contact angle measurements. Contact angles of the membranes were measured with a deionized water droplet of 3.0 μL on membrane surface adopting a contact angle goniometer (JC2000C Contact Angle Meter, China). A high-speed camera was used to capture the instantaneous water contact angle of the membranes. Five membrane samples were measured and the values reported were averaged.

Zeta potential. The surface zeta potential of the membranes was performed by a SurPASS electrokinetic analyzer (Anton Paar KG, Austria) at room temperature (25±1 ^{o}C). For each measurement, the membrane samples (1 cm × 0.5 cm) were attached to a holder to contact with 1 mmol L^{-1} KCl solution (pH=6.0±0.2). Each membrane sample was tested at least five times to obtain an average value.

2. Figures

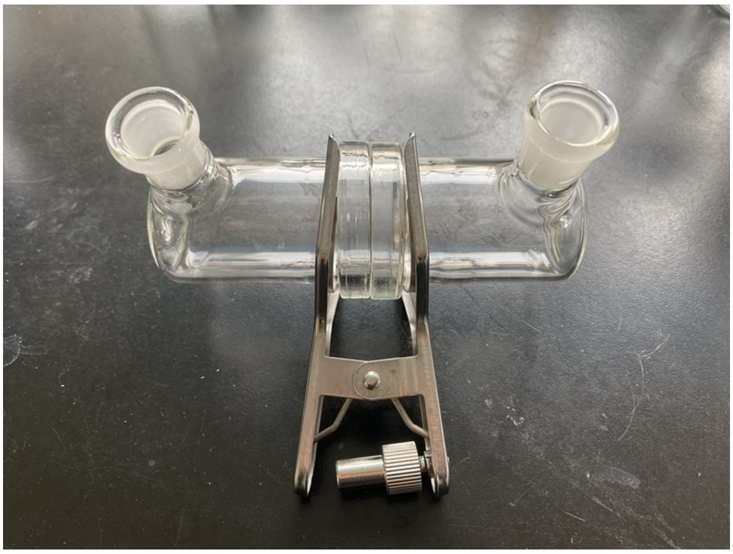

Fig. S1 Home-made diffusion cell.

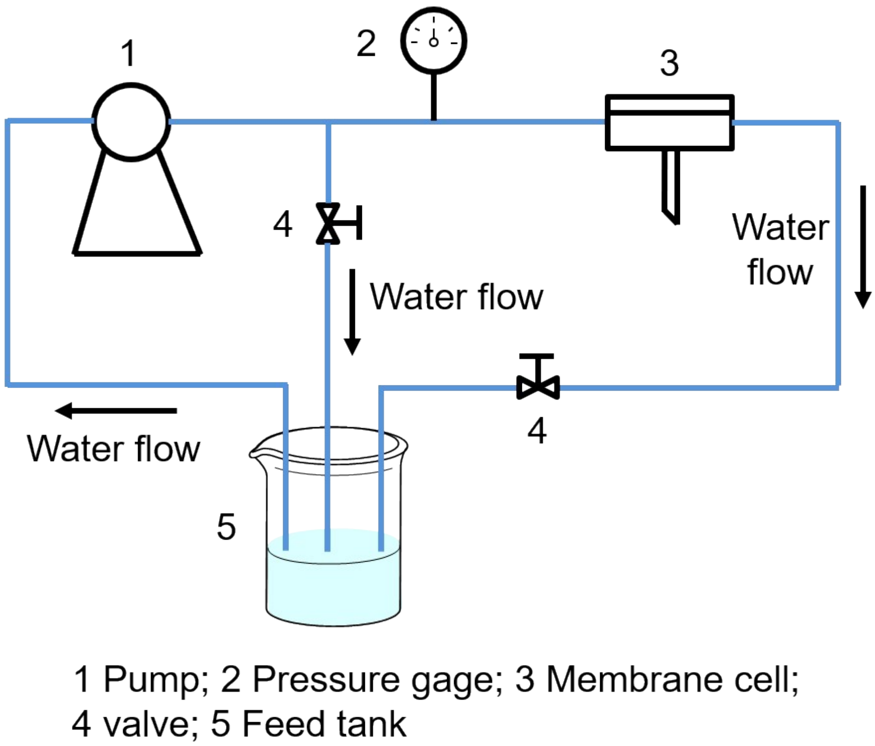

Fig. S2 Cross-flow filtration system for evaluating desalination performance of the membranes. Flow velocity: 45 L h^{-1}, driving pressure: 5.0 bar, effective filtration area: 3.14 cm^2.

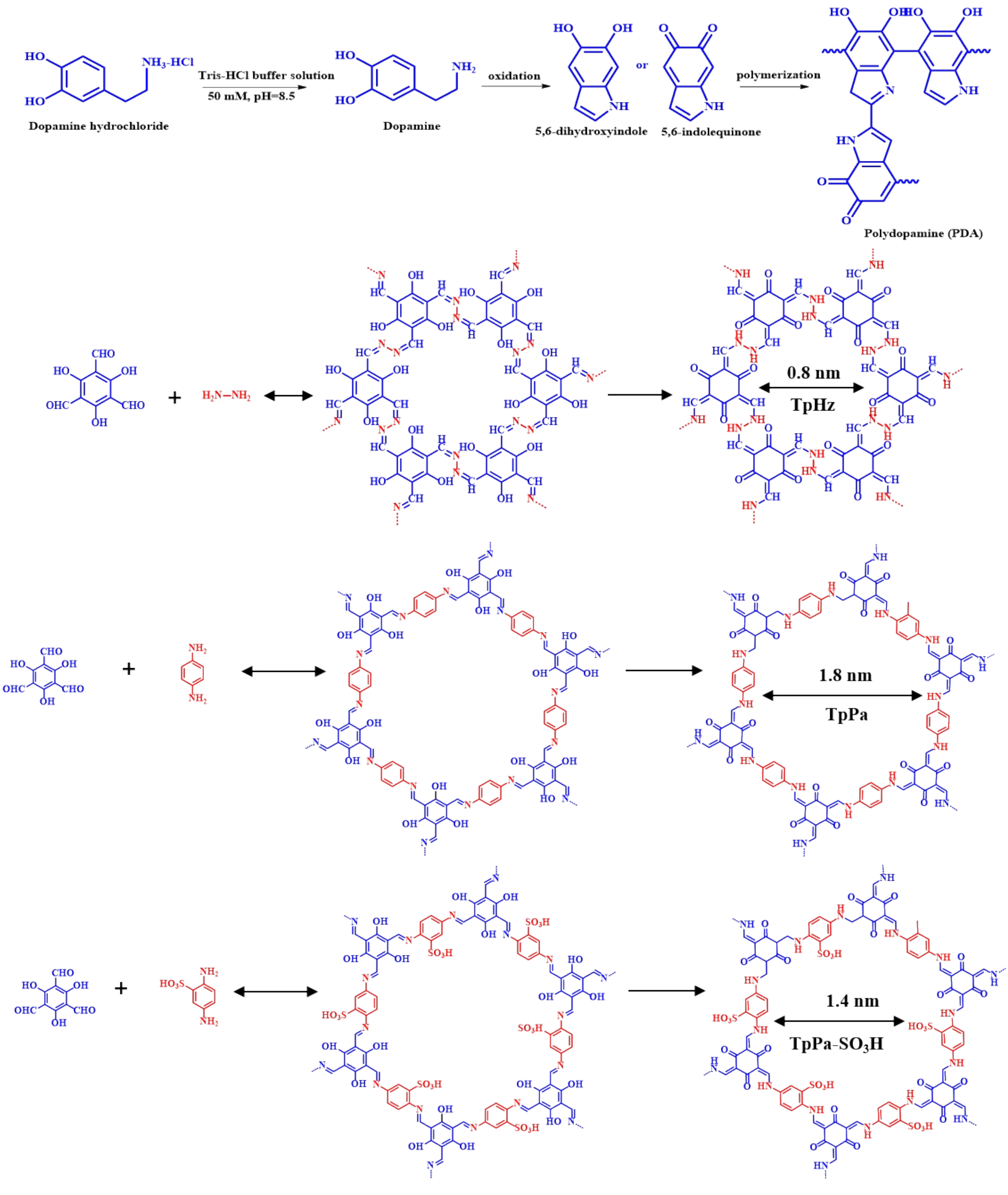

Fig. S3 Reaction route of polydopamine and COFs.

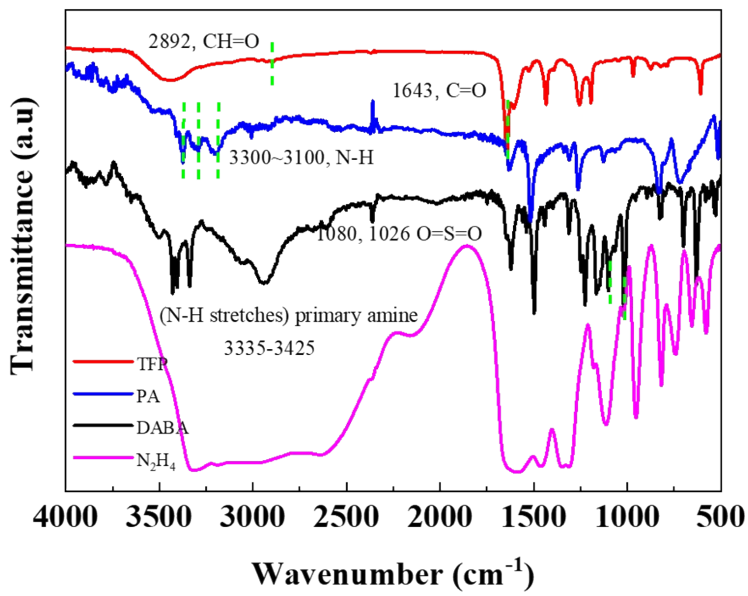

Fig. S4 FTIR spectrum of the building monomers.

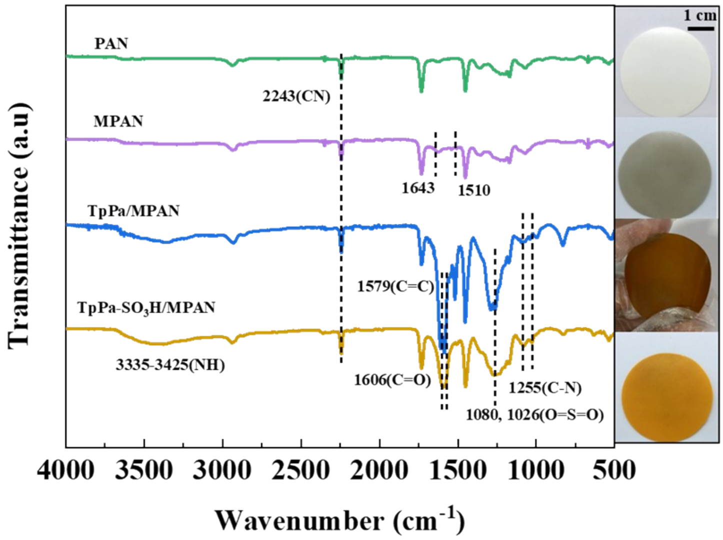

Fig. S5 ATR-FTIR spectrum of the supports and COF membranes with single layer. From top to bottom: PAN support, MPAN support, TpPa/MPAN and TpPa-SO_3H/MPAN membranes.

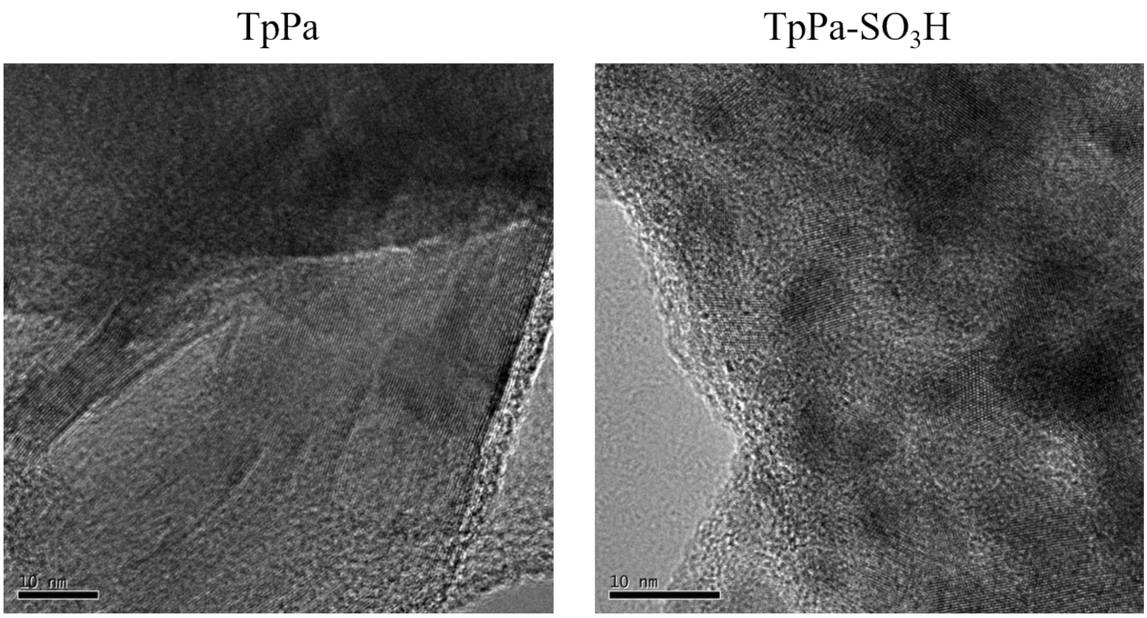

Fig. S6 High-resolution TEM of TpPa and TpPa-SO_3H nanofilms.

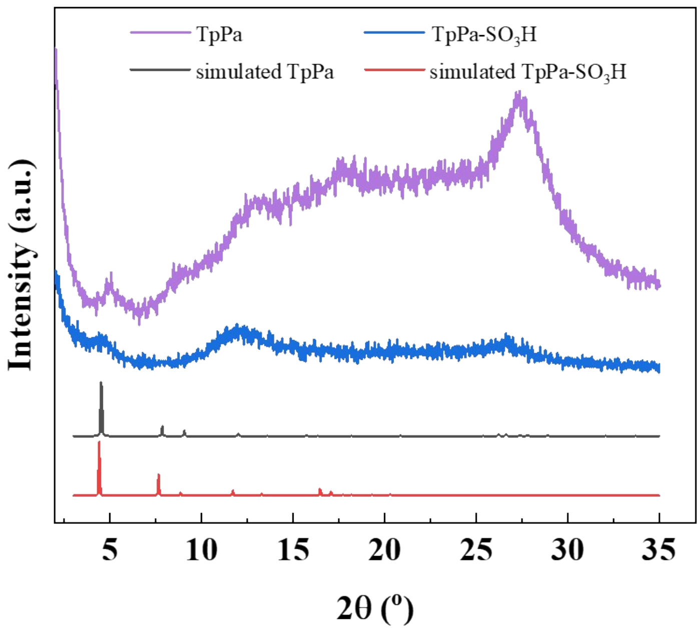

Fig. S7 XRD pattern of the single layer COF membranes and the simulated COFs.

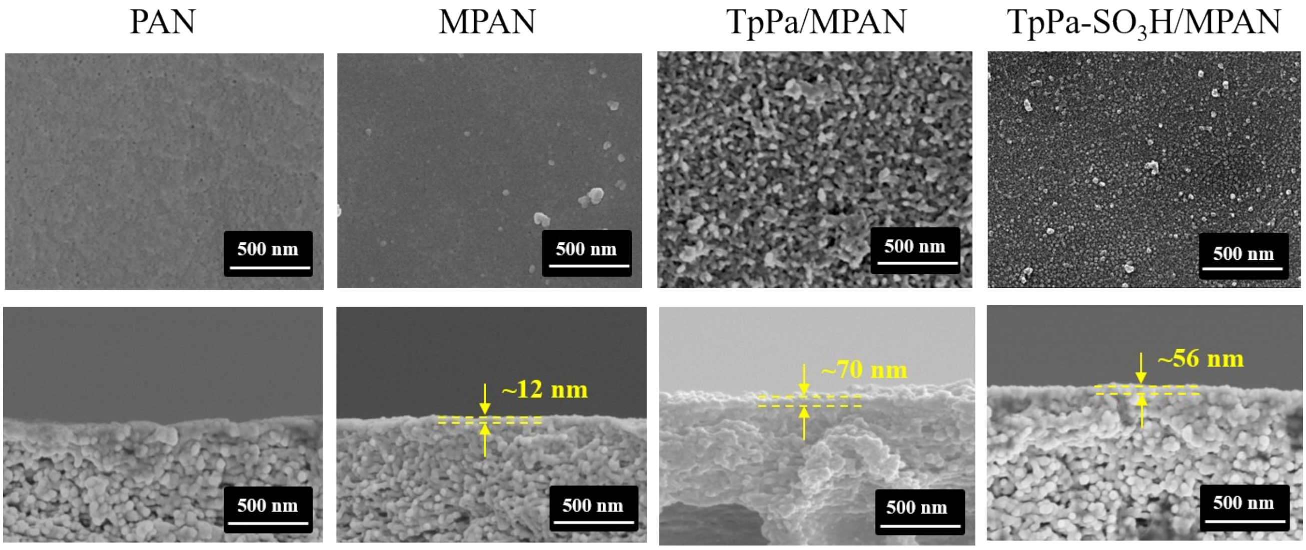

Fig. S8 Surface and cross-sectional SEM images of the membranes.

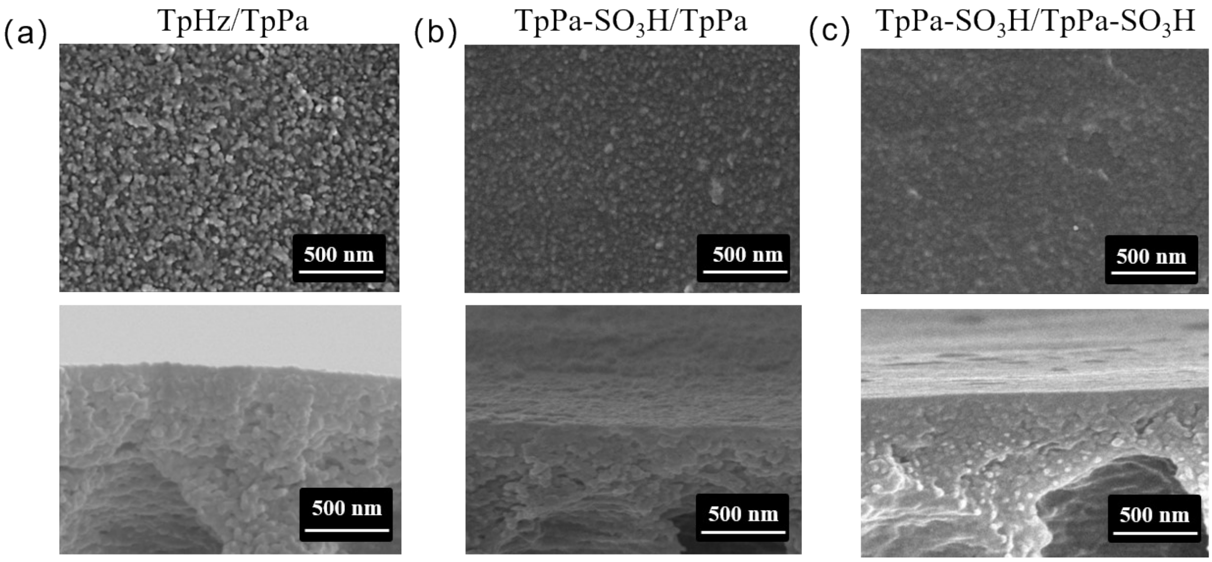

Fig. S9 Surface and cross-sectional SEM images of the bilayer COF membranes.

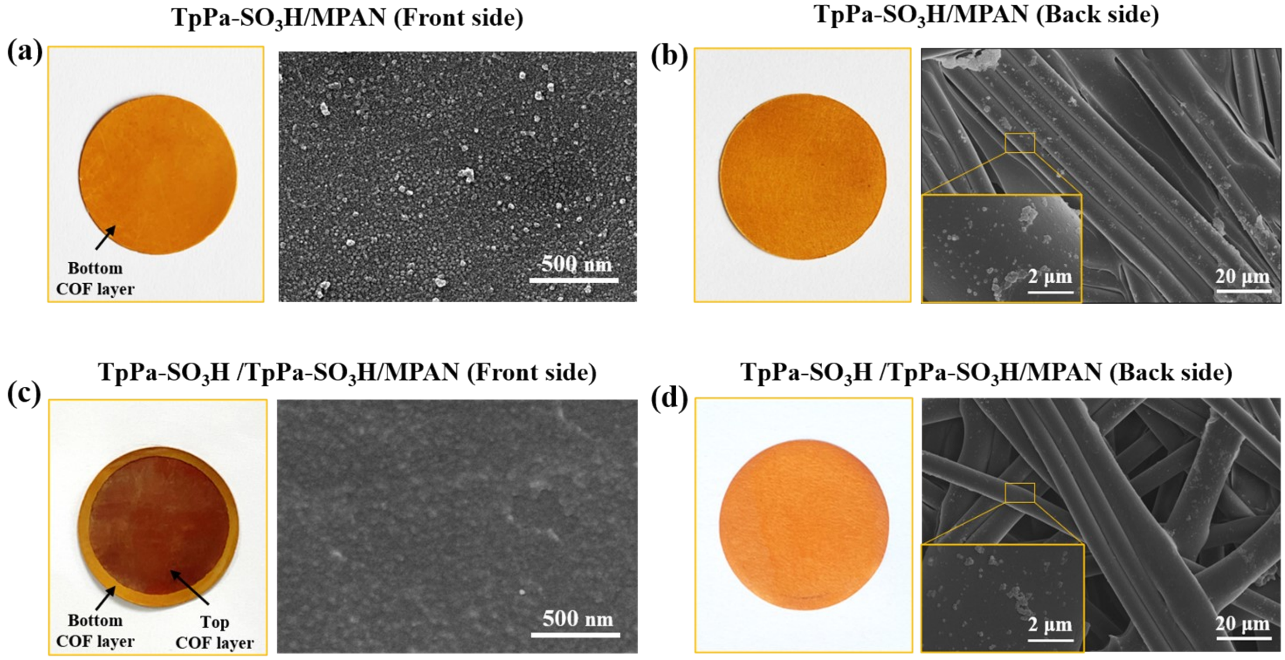

Fig. S10 The digital photographs (left) and surface SEM images (right) of the top side of TpPa-SO_3H/MPAN (a) and TpPa-SO_3H/TpPa-SO_3H/MPAN (c). The digital photographs (left) and surface SEM images (right) of the bottom side of TpPa-SO_3H/MPAN (b) and TpPa-SO_3H/TpPa-SO_3H/MPAN (d). Insets show an image at a higher magnification.

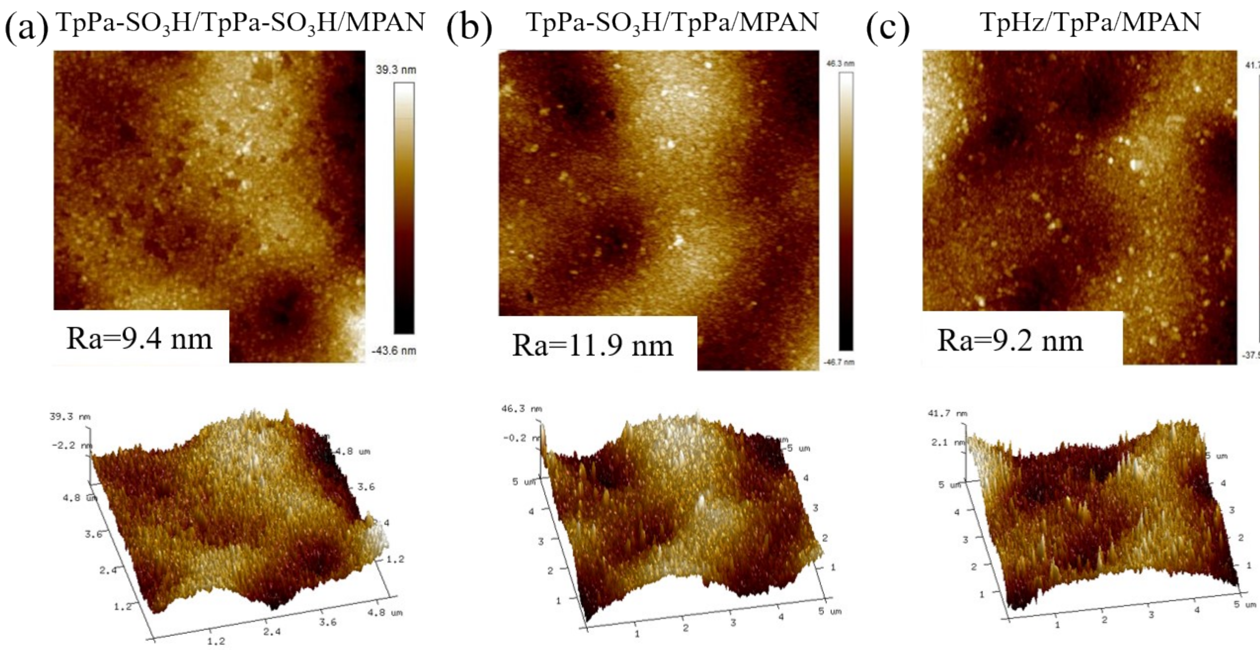

Fig. S11 AFM topography of bilayer COF membranes. Scanning area: 5 μm by 5 μm.

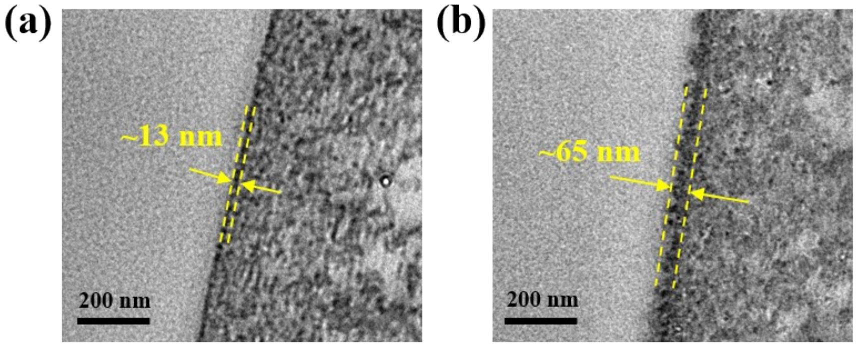

Fig. S12 Cross-sectional TEM images of (a) MPAN support, (b) TpPa/MPAN membrane.

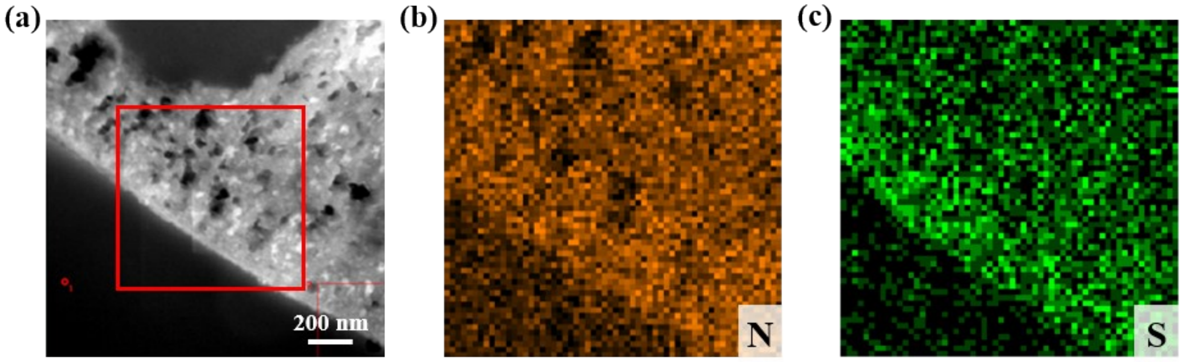

Fig. S13 (a) Dark-field cross-sectional TEM images and corresponding element maps of (b) N, (c) S of TpPa-SO_3H/TpPa/MPAN membrane.

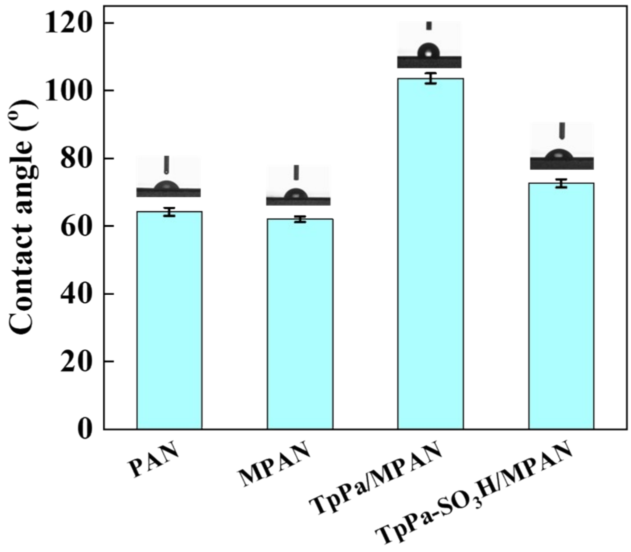

Fig. S14 Water contact angle of the supports and COF membranes with single layer.

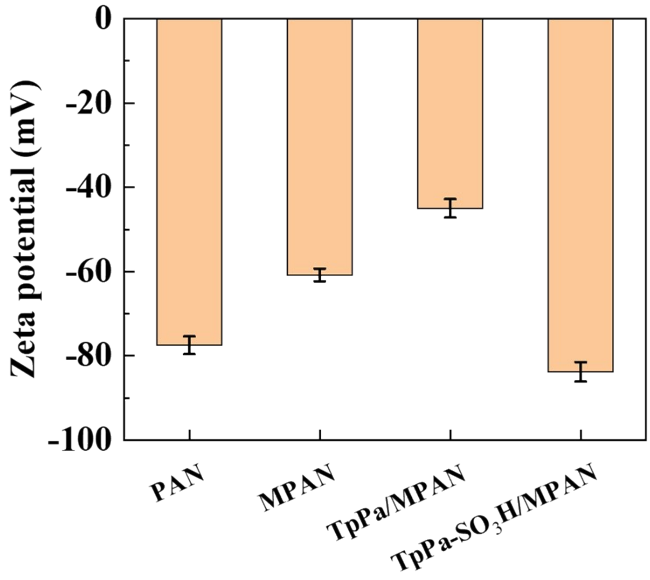

Fig. S15 Zeta potential of the supports and COF membranes with single layer.

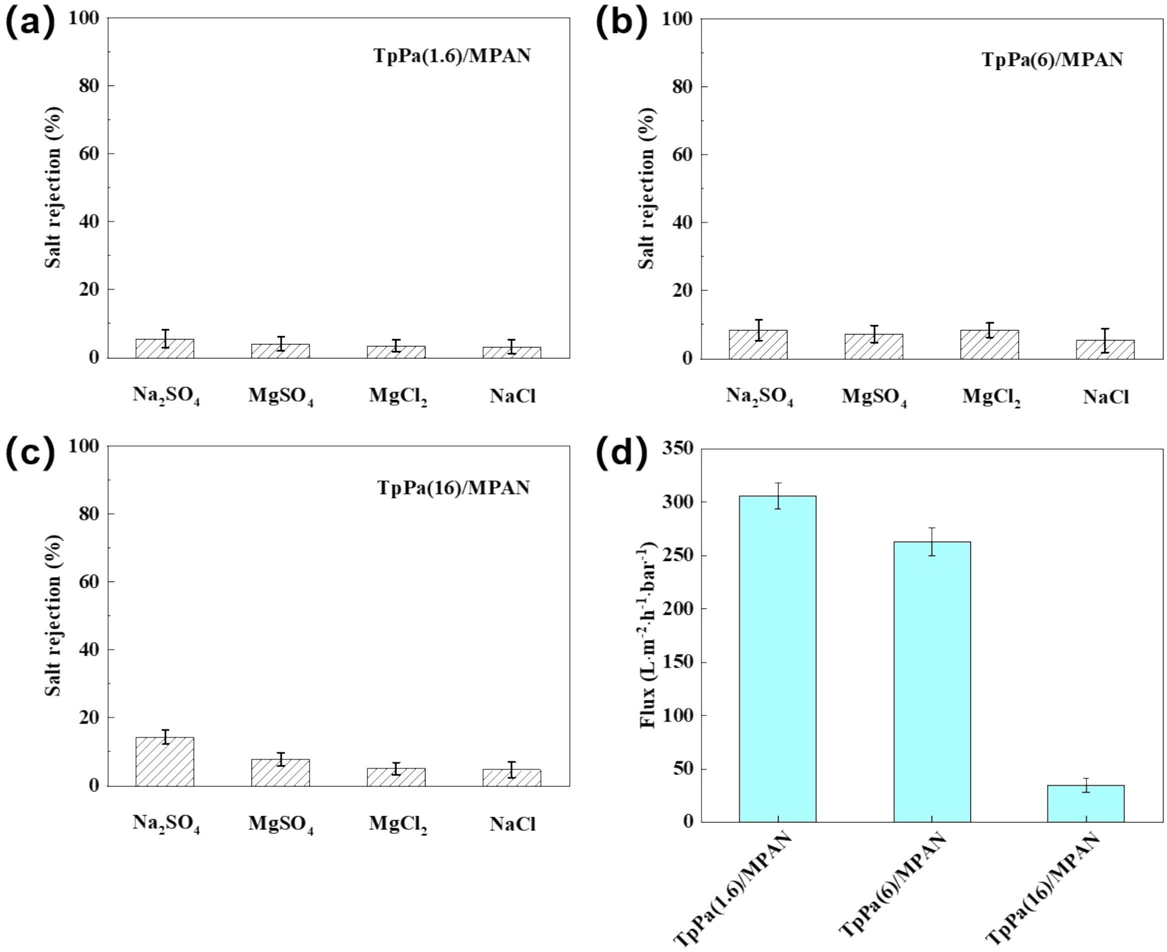

Fig. S16 Salt rejection of (a-c) and water flux (d) of TpPa/MPAN membranes prepared *via in situ* growth technique at room temperature.

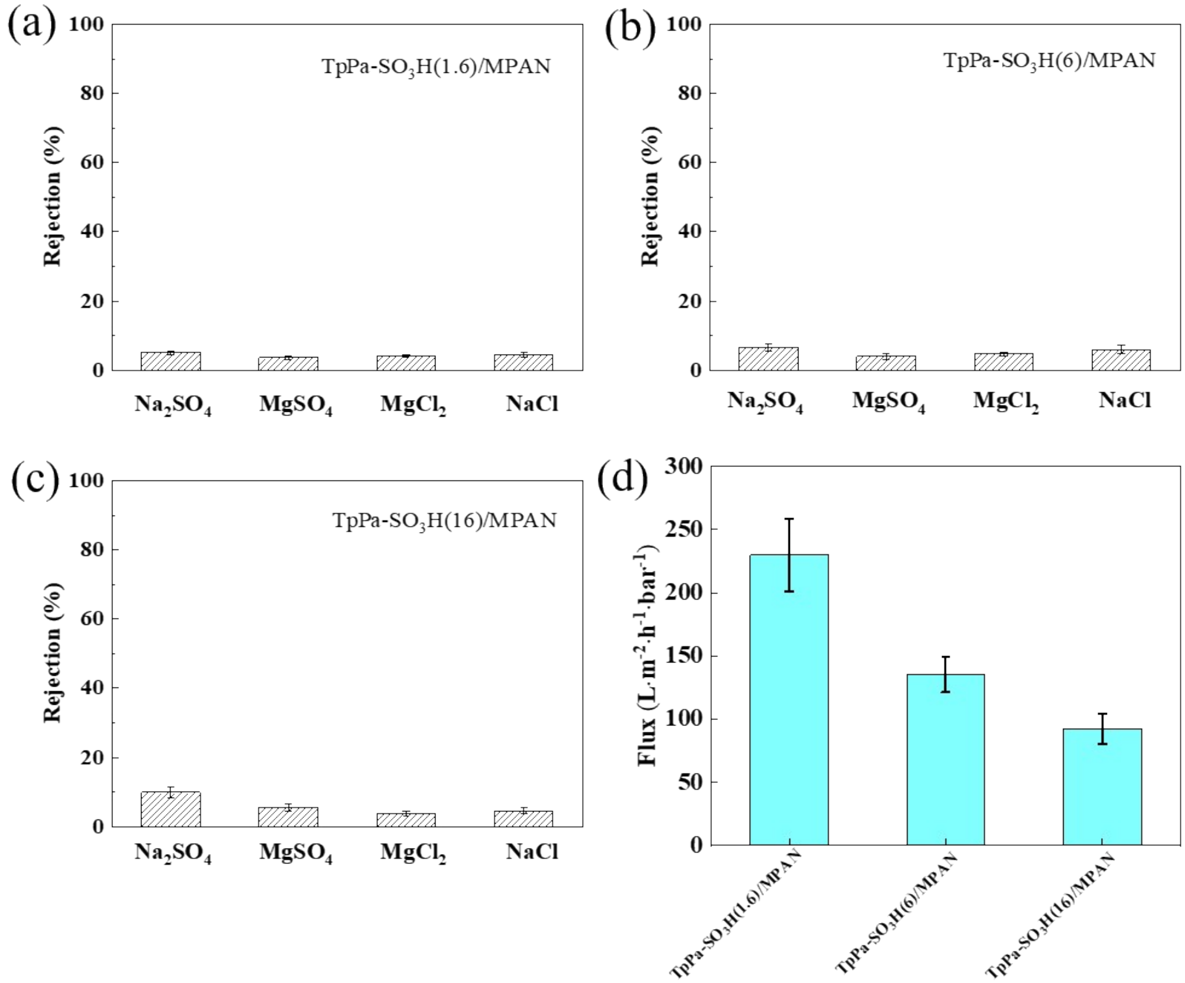

Fig. S17 Salt rejection (a-c) and water flux (d) of TpPa-SO_3H/MPAN membranes prepared *via in situ* growth technique at room temperature.

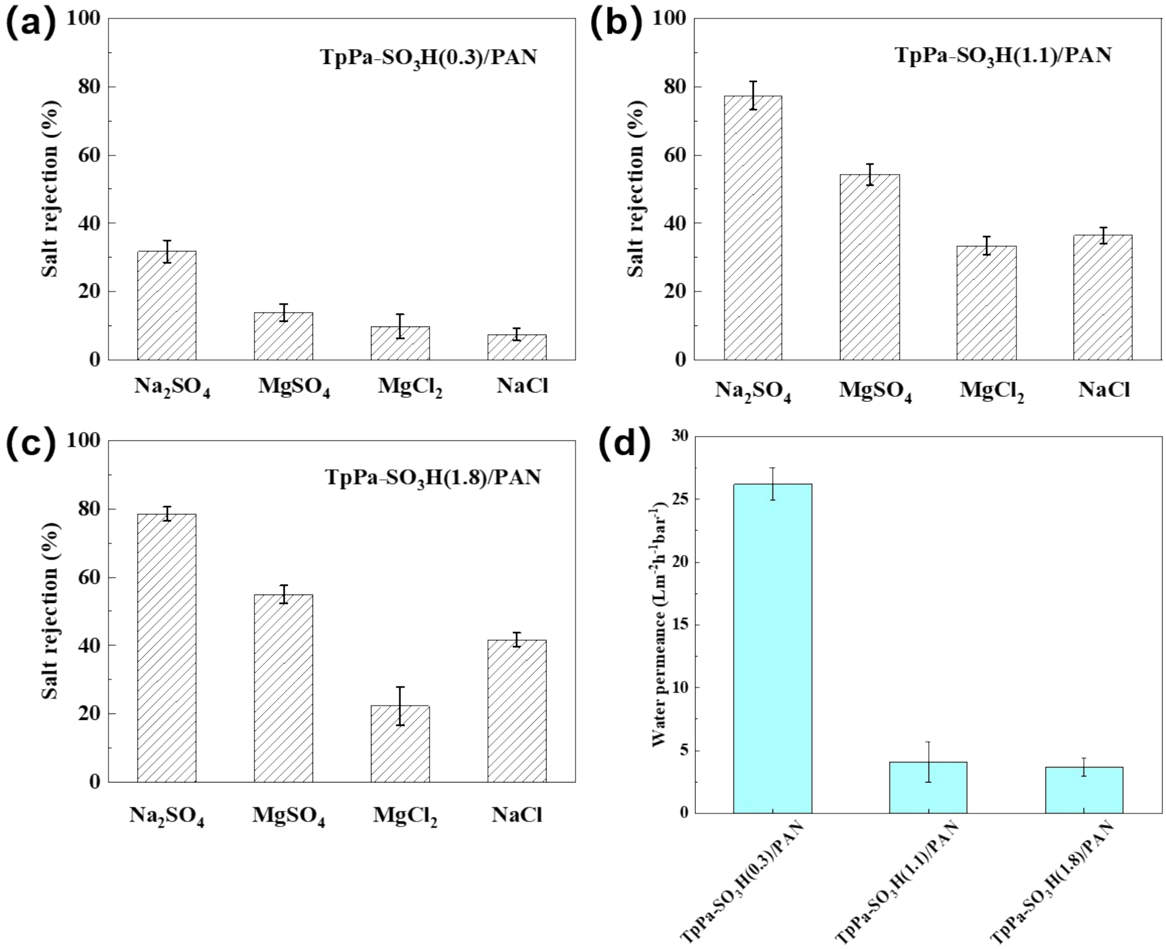

Fig. S18 Effect of monomer concentration on (a-c) salt rejection and (d) water permeance of TpPa-SO_3H/PAN membranes prepared by counter-diffusion approach under room temperature.

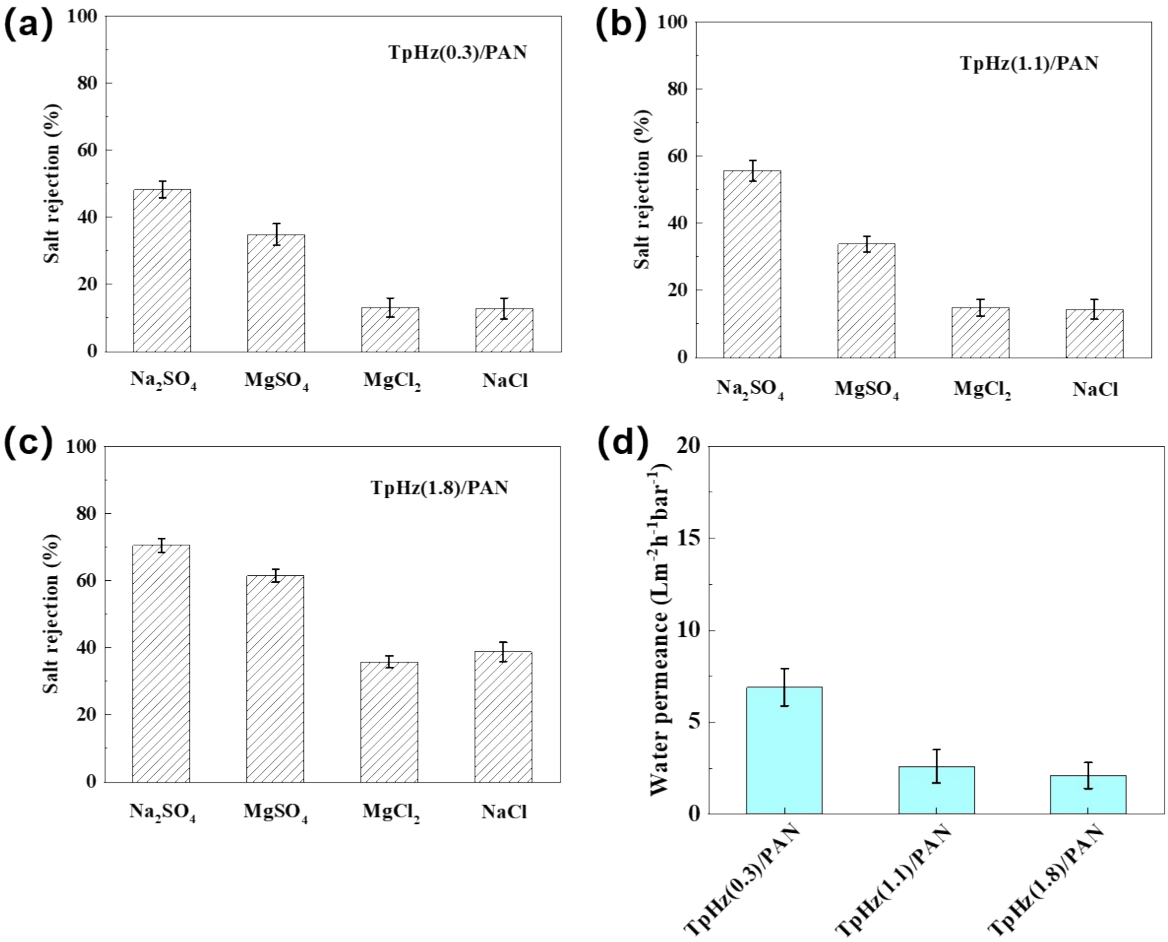

Fig. S19 Effect of monomer concentration on (a-c) salt rejection and (d) water permeance of TpHz/PAN membranes prepared by counter-diffusion approach under room temperature.

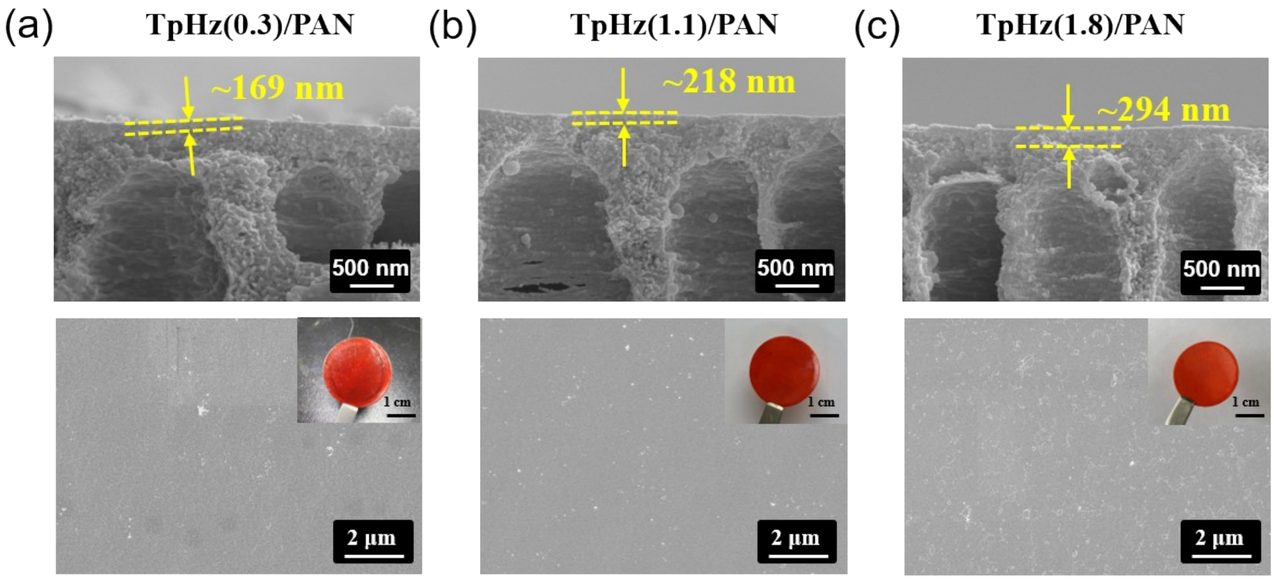

Fig. S20 SEM images of the TpHz/PAN membranes prepared via counter-diffusion approach under room temperature.

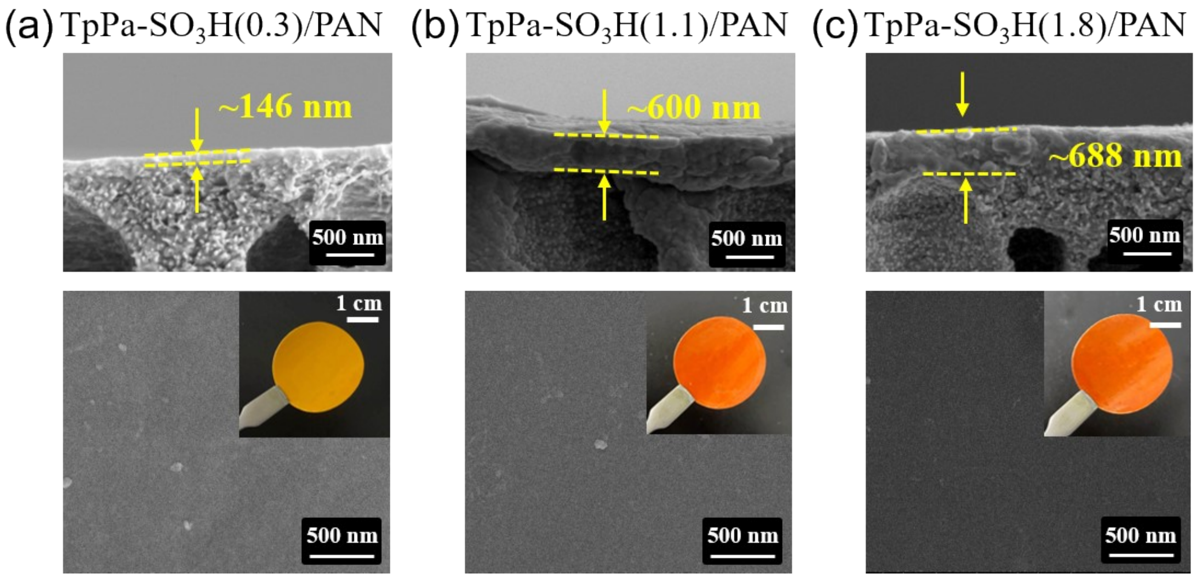

Fig. S21 SEM images of the TpPa-SO_3H/PAN membranes prepared via counter-diffusion approach under room temperature.

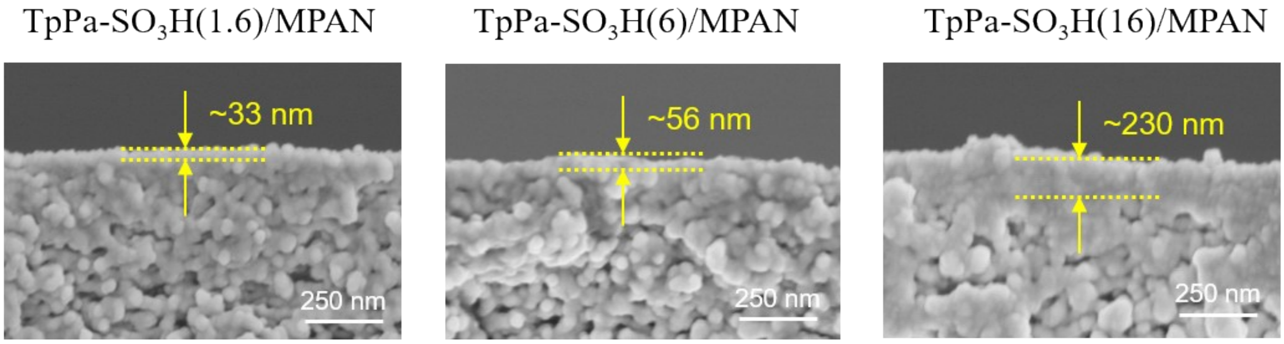

Fig. S22 Cross-sectional SEM images of the TpPa-SO_3H/MPAN membranes prepared via *in situ* growth under room temperature.

TpPa-SO_3H(1.1)/TpPa-SO_3H(1.6) TpPa-SO_3H(1.1)/TpPa-SO_3H(6) TpPa-SO_3H(1.1)/TpPa-SO_3H(16)

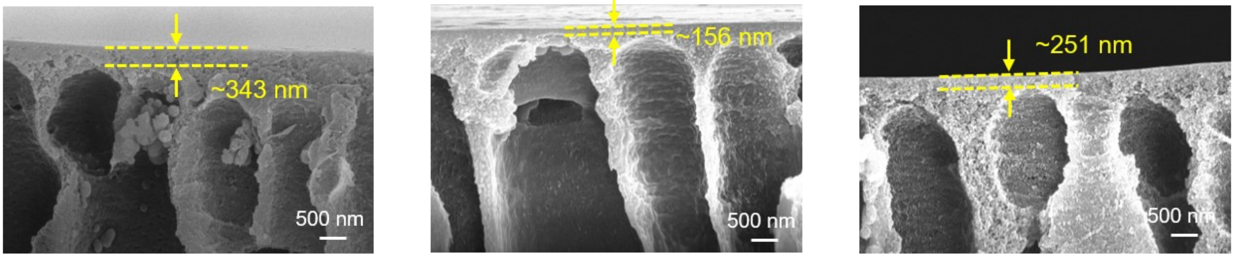

Fig. S23 Cross-sectional SEM images of the homointerface TpPa-SO_3H/TpPa-SO_3H/MPAN membranes.

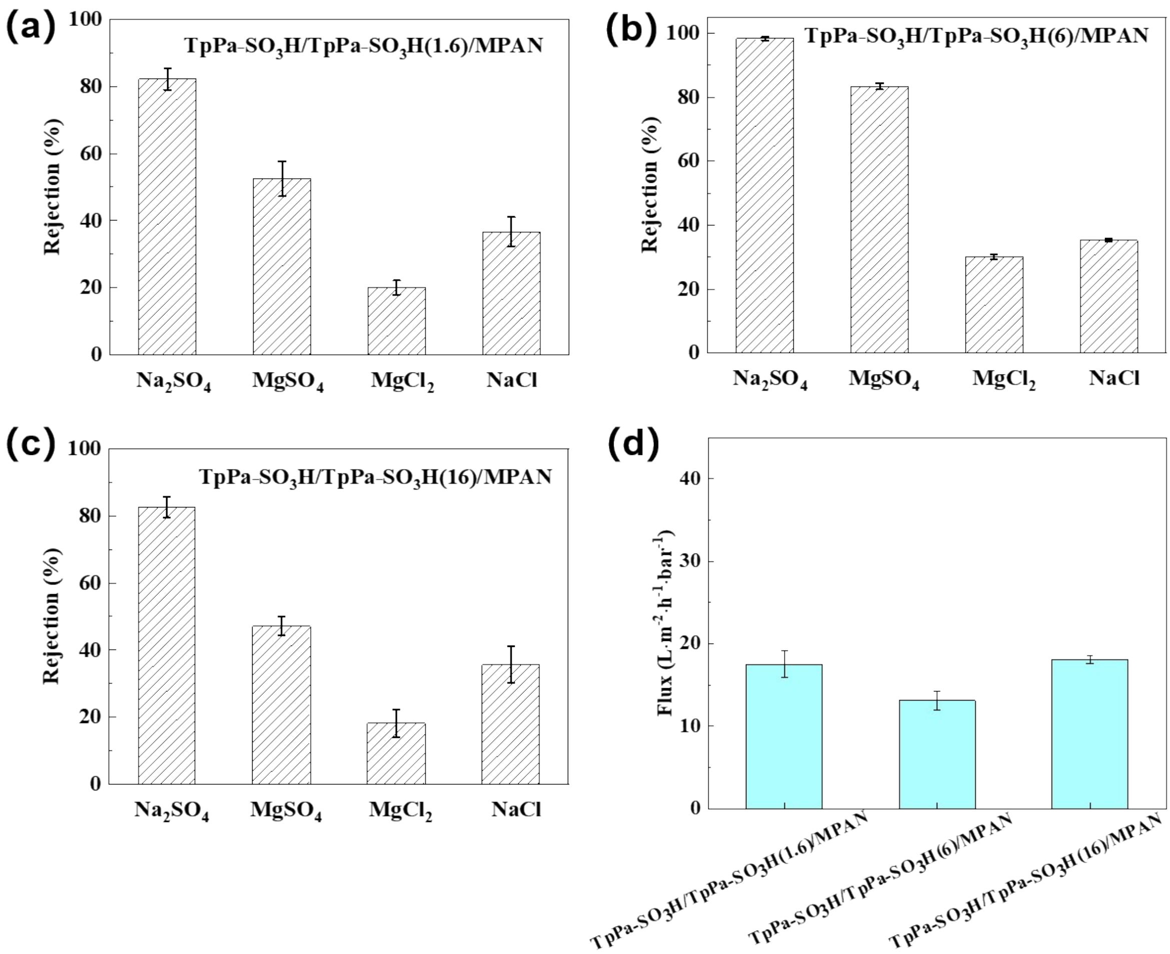

Fig. S24 Effect of monomer concentration on (a-c) salt rejection and (d) water permeance of homointerface TpPa-SO_3H(1.1)/TpPa-SO_3H/MPAN membranes.

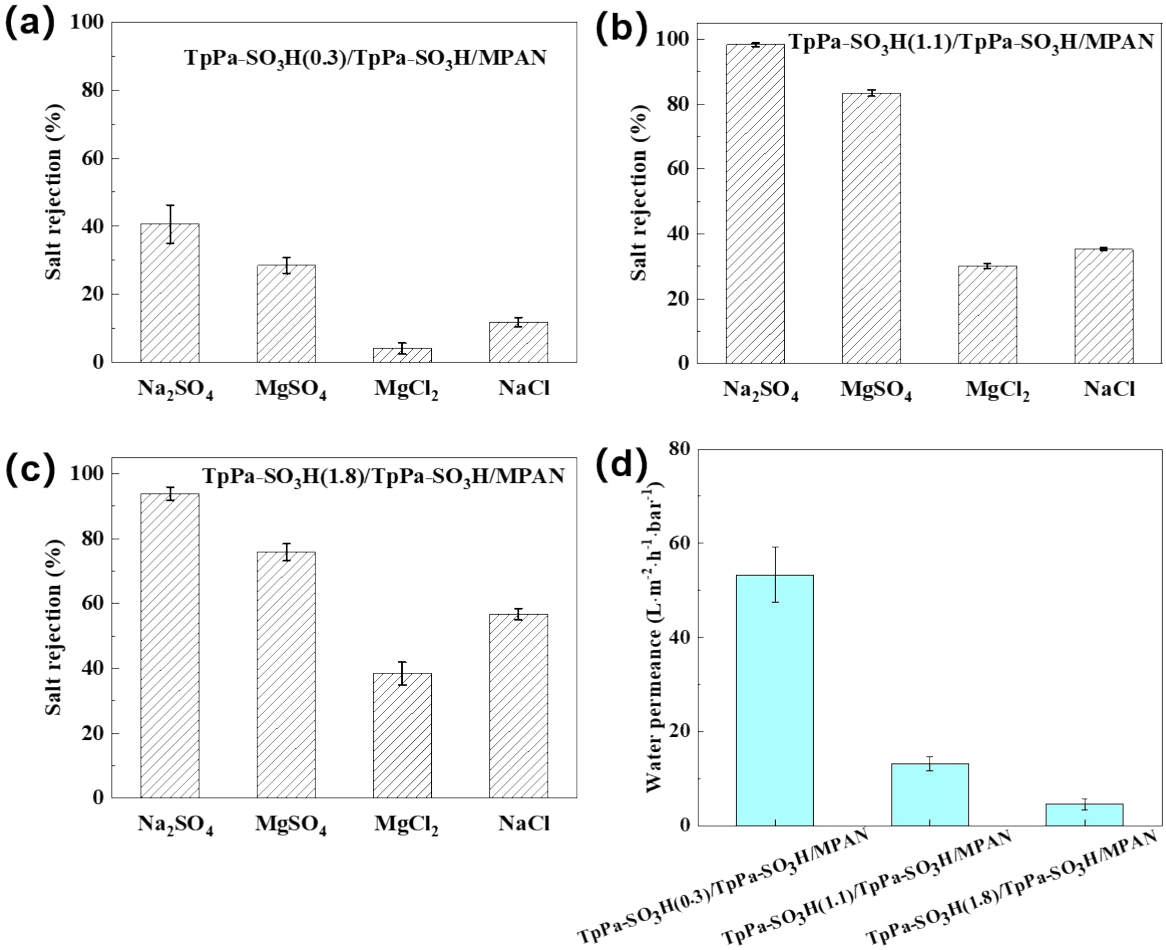

Fig. S25 Effect of monomer concentration on (a-c) salt rejection and (d) water permeance of homointerface TpPa-SO_3H/TpPa-SO_3H(6)/MPAN membranes.

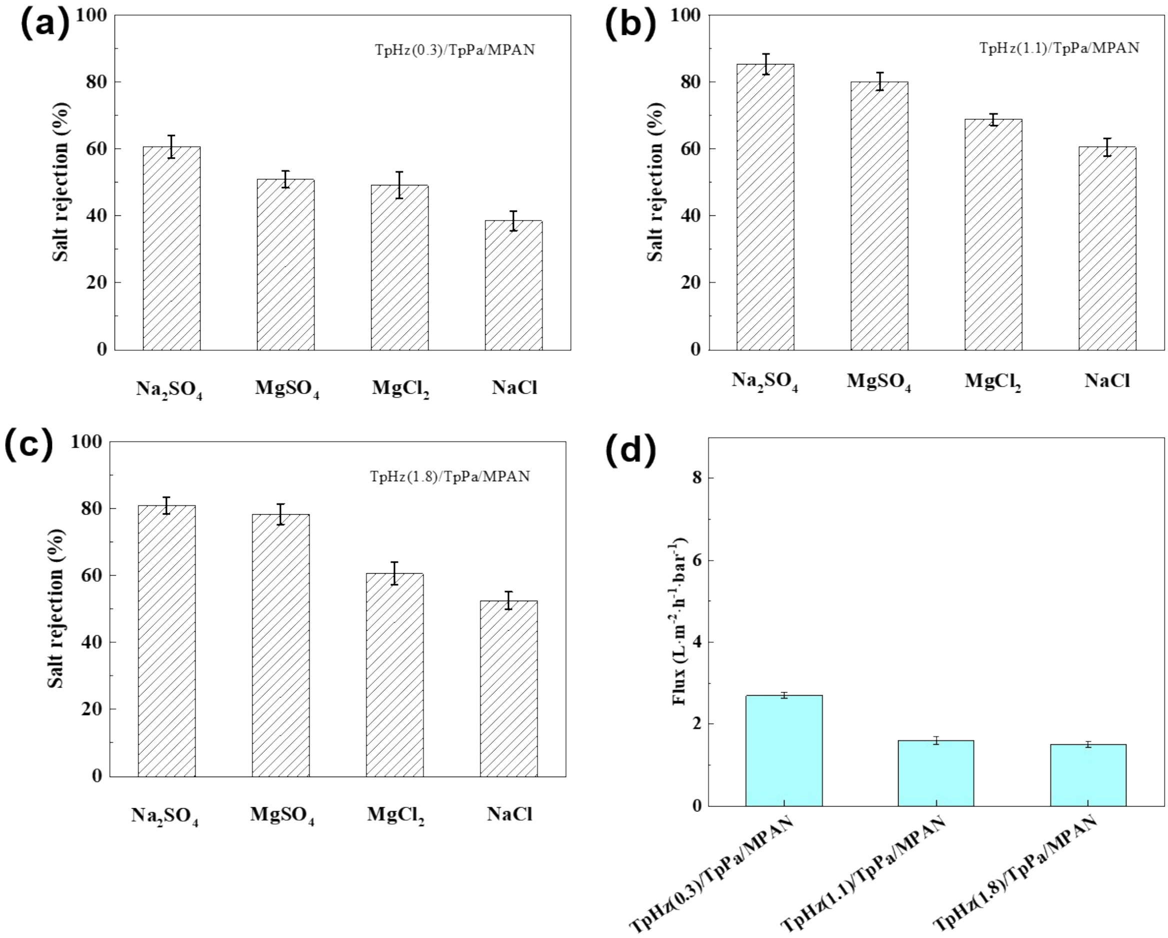

Fig. S26 Effect of monomer concentration on (a-c) salt rejection and (d) water permeance of homointerface TpHz/TpPa(6)/MPAN membranes.

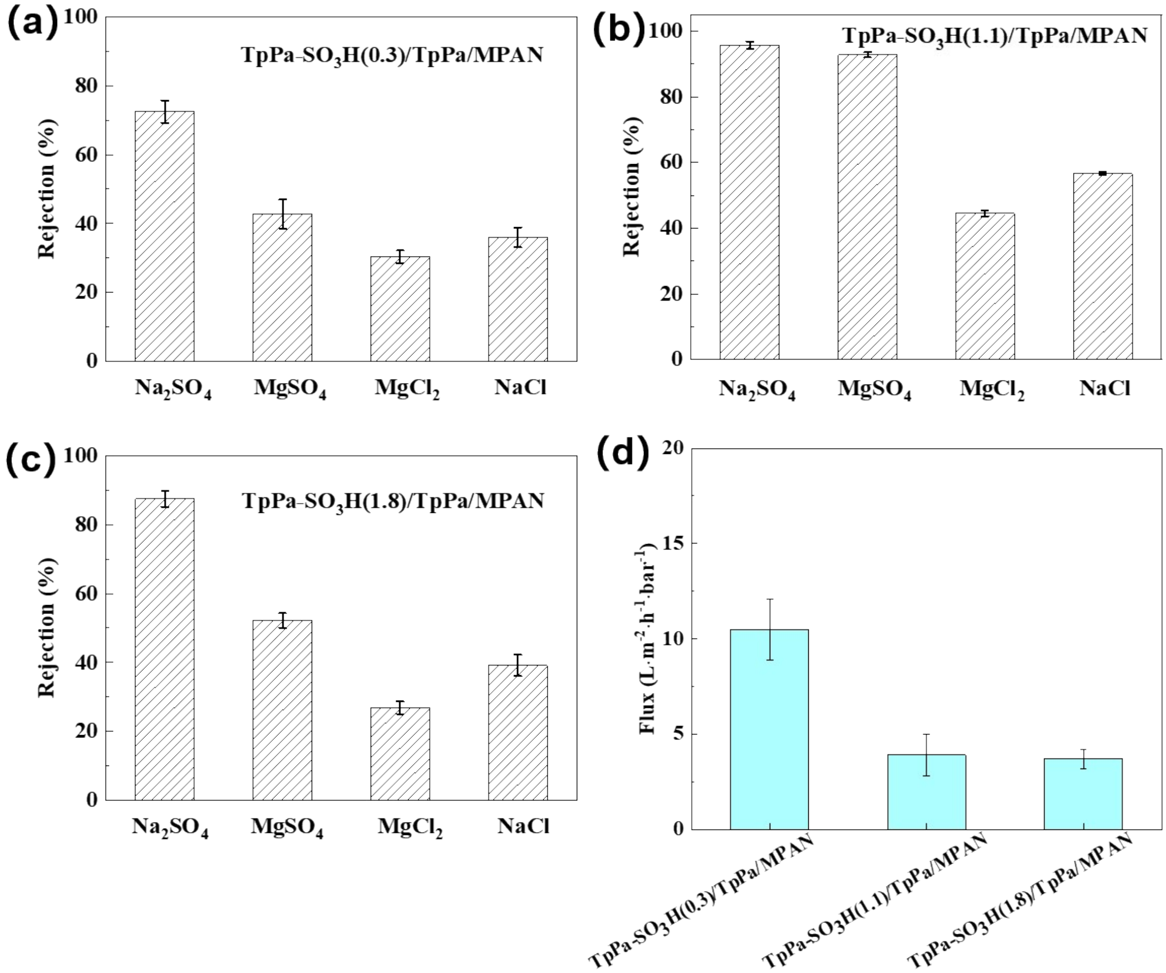

Fig. S27 Effect of monomer concentration on (a-c) salt rejection and (d) water permeance of homointerface TpPa-SO_3H/TpPa(6)/MPAN membranes.

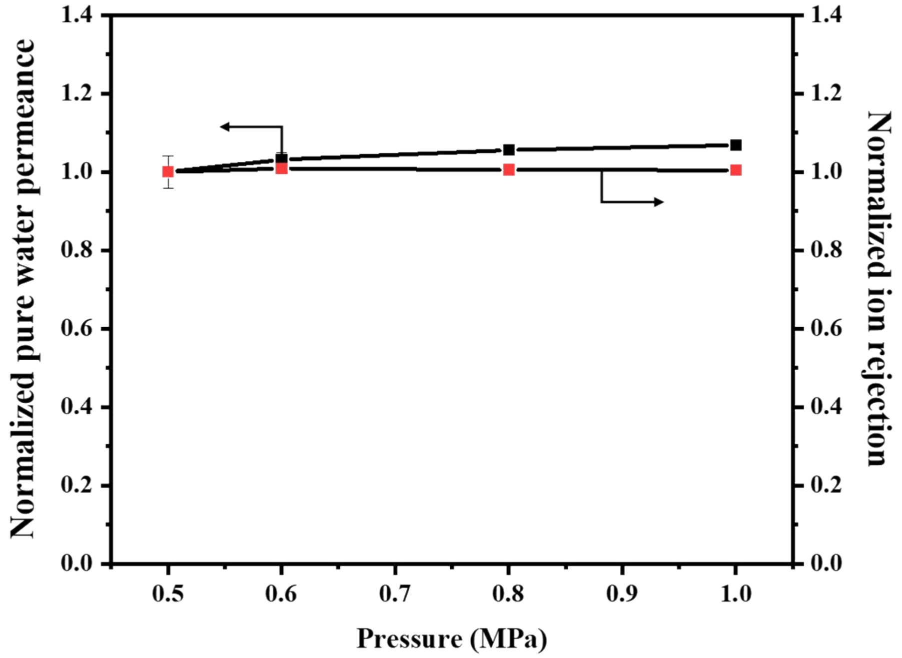

Fig. S28 The water permeance and Na_2SO_4 rejection of the bilayer COF membranes (TpPa-SO_3H/TpPa-SO_3H/MPAN) under high pressure.

3. Tables

Table S1. Single layer COF membranes prepared with various monomer concentrations.

Membrane	PDA deposition time (h)	COF building monomers		
		PA concentration (mmol L^{-1})	DABA concentration (mmol L^{-1})	TFP concentration (mmol L^{-1})
TpPa(1.6)/MPAN	1	2.4	/	1.6
TpPa(6)/MPAN	1	9	/	6
TpPa(16)/MPAN	1	24	/	16
TpPa-SO_3H(1.6)/MPAN	1	/	2.4	1.6
TpPa-SO_3H(6)/MPAN	1	/	9	6
TpPa-SO_3H(16)/MPAN	1	/	24	16

Table S2. Bilayer COF membranes prepared with different building monomers.

Membrane	Monomer concentration of COF bottom layer (mmol L^{-1})			Monomer concentration of COF top layer (mmol L^{-1})		
	PA	DABA	TFP	N_2H_4	DABA	TFP
TpHz(0.3)/TpPa(6)/MPAN	9.0	/	6.0	0.5	/	0.3
TpHz(1.1)/TpPa(6)/MPAN	9.0	/	6.0	1.7	/	1.1
TpHz(1.8)/TpPa(6)/MPAN	9.0	/	6.0	2.8	/	1.8
TpPa-SO_3H(0.3)/TpPa(6)/MPAN	9.0	/	6.0	/	0.5	0.3
TpPa-SO_3H(1.1)/TpPa(6)/MPAN	9.0	/	6.0	/	1.7	1.1
TpPa-SO_3H(1.8)/TpPa(6)/MPAN	9.0	/	6.0	/	2.8	1.8
TpPa-SO_3H(1.1)/TpPa-SO_3H(1.6)/MPAN(1#)	/	2.4	1.6	/	1.7	1.1
TpPa-SO_3H(1.1)/TpPa-SO_3H(6)/MPAN(2#)	/	9.0	6.0	/	1.7	1.1
TpPa-SO_3H(1.1)/TpPa-SO_3H(16)/MPAN(3#)	/	24	16	/	1.7	1.1
TpPa-SO_3H(0.3)/TpPa-SO_3H(6)/MPAN	/	9.0	6.0	/	0.5	0.3
TpPa-SO_3H(1.1)/TpPa-SO_3H(6)/MPAN	/	9.0	6.0	/	1.7	1.1
TpPa-SO_3H(1.8)/TpPa-SO_3H(6)/MPAN	/	9.0	6.0	/	2.8	1.8

Table S3. Spherical neutral solutes with various molecular weights were selected for rejection tests.

Solutes	Molecular structure	Molecular Weight (Da)	Stokes radius (nm)[2]	Rejection (%)		
				TpHz/TpPa /MPAN	TpPa-SO_3H/TpPa/ MPAN	TpPa-SO_3H/TpPa-SO_3H/MPAN
Isobutanol	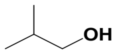	74.1	0.279	28.4±1.4	15.2±1.8	12.0±2.0
Glucose	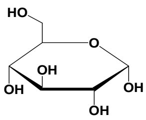	180.1	0.358	60.3±2.1	53.5±2.2	45.4±2.6
Sucrose	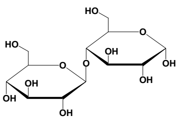	342.2	0.462	83.2±3.2	78.0±3.1	77.0±3.3
Raffinose	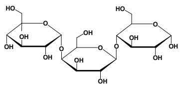	504.4	0.584	89.0±2.7	86.1±1.2	85.1±1.7
β-cyclodextrin	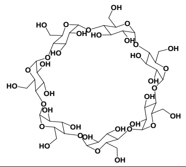	1135.0	0.742	95.7±2.4	96.4±3.5	93.0±2.5

A series of spherical neutral solutes (isobutanol, glucose, sucrose, raffinose and β-cyclodextrin) were used to estimate the MWCO of the bilayer COF membranes. The rejection rate of 90% is regarded as the MWCO of the membrane. Each solution (100 ppm) was recycled by a home-made cross-flow apparatus at 5.0 bar. The rejection of the solutes was calculated based on equation (1) below, where the concentrations of the permeate (C_p) and feed (C_f) were measured by a total organic carbon (TOC, HTY-CT1000A, China) analyzer.

$$R = \frac{C_f - C_p}{C_f} \times 100\% \tag{1}$$

The average pore size of the bilayer COF membranes equals the Stokes radius of the spherical solute when the rejection rate reaches 50%. The aperture distribution is expressed as a probability density function and is derived from equation 2 below [1-3]:

$$\frac{dR(r_p)}{dr_p} = \frac{1}{r_p \ln \sigma_p \sqrt{2\pi}} \exp\left[-\frac{(\ln r_p - \ln \mu_p)^2}{2(\ln \sigma_p)^2} \right] \tag{2}$$

where r_p refers to Stokes radius of the spherical neutral solute, σ_p refers to the ratio of solute radius at R_p=84.13% to

50.0%, μ_p refers to the average pore size calculated from Stokes radius of the solutes, respectively.

Table S4. Performance comparison of various COF membranes towards salt rejection.

Membrane	salt	Permeance ($L\ m^{-2}\ h^{-1}\ MPa^{-1}$)	Rejection (%)	Operation pressure (MPa)	Ref.
FS-COM-1	Na_2SO_4	38.6	90-95	0.1	[4]
IISERP-COOH-COF1	Na_2SO_4	5	96.3	0.2	[5]
TpHz/PES	Na_2SO_4	40.5	58.3	0.4	[6]
COF-LZU1	Na_2SO_4	760	3.2	0.5	[7]
COF-LZU1/HPAN	Na_2SO_4	442	63.6	0.2	[8]
TpPa-1/HPAN	Na_2SO_4	418.5	15	0.1	[9]
COF-LZU1/PES	Na_2SO_4	800	10.8	0.2	[10]
ACOF-1	Na_2SO_4	5.6	95.7	0.3	[11]
TpHz/TpPa/MPAN	Na_2SO_4	16	85.4	0.5	This work
TpPa-SO_3H/TpPa/MPAN	Na_2SO_4	39	95.7	0.5	
TpPa-SO_3H/TpPa-SO_3H/MPAN	Na_2SO_4	131	98.3	0.5	

4. References

[1] J. Gao, S. Sun, W. Zhu and T. Chung, *J. Membr. Sci.*, 2014, 452, 300-310.

[2] Y. Liang, Y. Zhu, C. Liu, K. Lee, W. Hung, Z. Wang, Y. Li, M. Elimelech, J. Jin and S. Lin, *Nat. Commun.*, 2020, 11, 2015.

[3] Y. Li, X. You, Y. Li, J. Yuan, J. Shen, R. Zhang, H. Wu, Y. Su and Z. Jiang, *J. Mater. Chem. A*, 2020, 8, 23930-23938.

[4] Y. Li, Q. Wu, X. Guo, M. Zhang, B. Chen, G. Wei, X. Li, X. Li, S. Li and L. Ma, *Nat. Commun.*, 2020, 11, 1-9.

[5] C. Liu, Y. Jiang, A. Nalaparaju, J. Jiang and A. Huang, *J. Mater. Chem. A*, 2019, 7, 24205-24210.

[6] R. Wang, M. Wei and Y. Wang, *J. Membr. Sci.*, 2020, 604, 118090.

[7] H. Fan, J. Gu, H. Meng, A. Knebel and J. Caro, *Angew. Chem. Int. Ed.*, 2018, 57, 4083-4087.

[8] C. Yin, S. Fang, X. Shi, Z. Zhang and Y. Wang, *J. Membr. Sci.*, 20201, 618, 118727.

[9] F. Pan, W. Guo, Y. Su, N. Khan, H. Yang and Z. Jiang, *Sep. Purif. Technol.*, 2019, 215, 582-589.

[10] Y. Su, X. Yan, Y. Chen, X. Guo, X. Chen and W. Lang, *J. Membr. Sci.*, 2021, 618, 118706.

[11] A. Xiao, X. Shi, Z. Zhang, C. Yin, S. Xiong and Y. Wang, *J. Membr. Sci.*, 2021, 624, 119122.